

pubs.acs.org/bc Communication

# DNA Nanostructures as Catalysts: Double Crossover Tile-Assisted 5' to 5' and 3' to 3' Chemical Ligation of Oligonucleotides

Andrea C. Bardales, Joseph R. Mills, and Dmitry M. Kolpashchikov\*



Cite This: Bioconjugate Chem. 2024, 35, 28-33



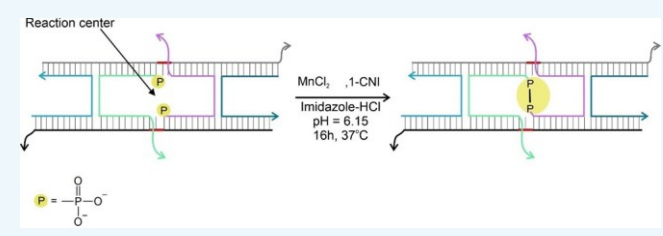
ACCES\$

III Metrics & More

Article Recommendations

Supporting Information

ABSTRACT: Accessibility of synthetic oligonucleotides and the success of DNA nanotechnology open a possibility to use DNA nanostructures for building sophisticated enzyme-like catalytic centers. Here we used a double DNA crossover (DX) tile nanostructure to enhance the rate, the yield, and the specificity of 5'-5' ligation of two oligonucleotides with arbitrary sequences. The ligation product was isolated via a simple procedure. The same strategy was applied for the synthesis of 3'-3' linked



oligonucleotides, thus introducing a synthetic route to DNA and RNA with a switched orientation that is affordable by a low-resource laboratory. To emphasize the utility of the ligation products, we synthesized a circular structure formed from intramolecular complementarity that we named "an impossible DNA wheel" since it cannot be built from regular DNA strands by enzymatic reactions. Therefore, DX-tile nanostructures can open a route to producing useful chemical products that are unattainable via enzymatic synthesis. This is the first example of the use of DNA nanostructures as a catalyst. This study advocates for further exploration of DNA nanotechnology for building enzyme-like reactive systems.

Protein enzymes facilitate chemical reactions by using multiple functional groups brought into proximity to specific substrates. Up to 10<sup>14</sup>-fold enhancement of the reaction rates is possible due to the simultaneous use of several catalytic strategies, including the proximity and orientation effect, preferential binding to the transition state, general acid/base, and electrophilic and nucleophilic catalysis. The proximity and orientation effect lowers the entropic barrier to form the transition state. This simple strategy has been explored in nucleic-acid-templated reactions, in which two reactive groups are conjugated to the opposite ends of two oligonucleotides and then brought together by hybridization.

Templated reactions have been used for the discovery of new chemical reactions,<sup>2</sup> DNA-triggered drug release,<sup>3</sup> DNA templated ligation,<sup>4</sup> and nucleic acid analysis,<sup>5</sup> among other applications.<sup>6</sup> The approaches, however, use B-DNA helix formation to bring into proximity the 3' end of one oligonucleotide to the 5' end of another in two major topological arrangements shown in Figure 1a. This strategy is limited by the requirement that the reactive groups be attached to the opposite DNA ends. Importantly, with B-DNA being a one-dimensional (1D) structure, it limits the number of reactive and/or catalytic groups that can be brought into proximity and leaves little room for achieving sophisticated enzyme-like architectures.

On the other hand, DNA nanotechnology has introduced non-natural 2D and 3D DNA nanostructures, such as an immobile four-way junction, paranemic crossover, and tensegrity triangle, to name a few. These blocks may allow the building of complex 3D arrangements of functional groups

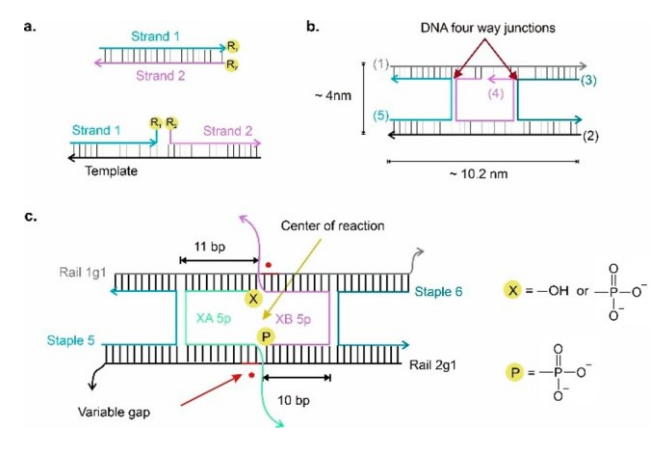


Figure 1. Topology of DNA-template-assisted and DX-tile-assisted reactions. (a) Conventional template-assisted reaction: strands 1 and 2 hybridize with each other or to a DNA template to bring the two reactive groups R1 and R2 into proximity, thus facilitating the reaction.<sup>2–6</sup> (b) Scheme of a DX tile developed by Fu and Seeman.<sup>11</sup> (c) Scheme of a DX tile designed in this study to catalyze the ligation of oligonucleotides at their 5′-phosphorylated termini.

Received: November 21, 2023 Revised: December 18, 2023 Accepted: December 20, 2023 Published: December 22, 2023





Bioconjugate Chemistry pubs.acs.org/bc Communication

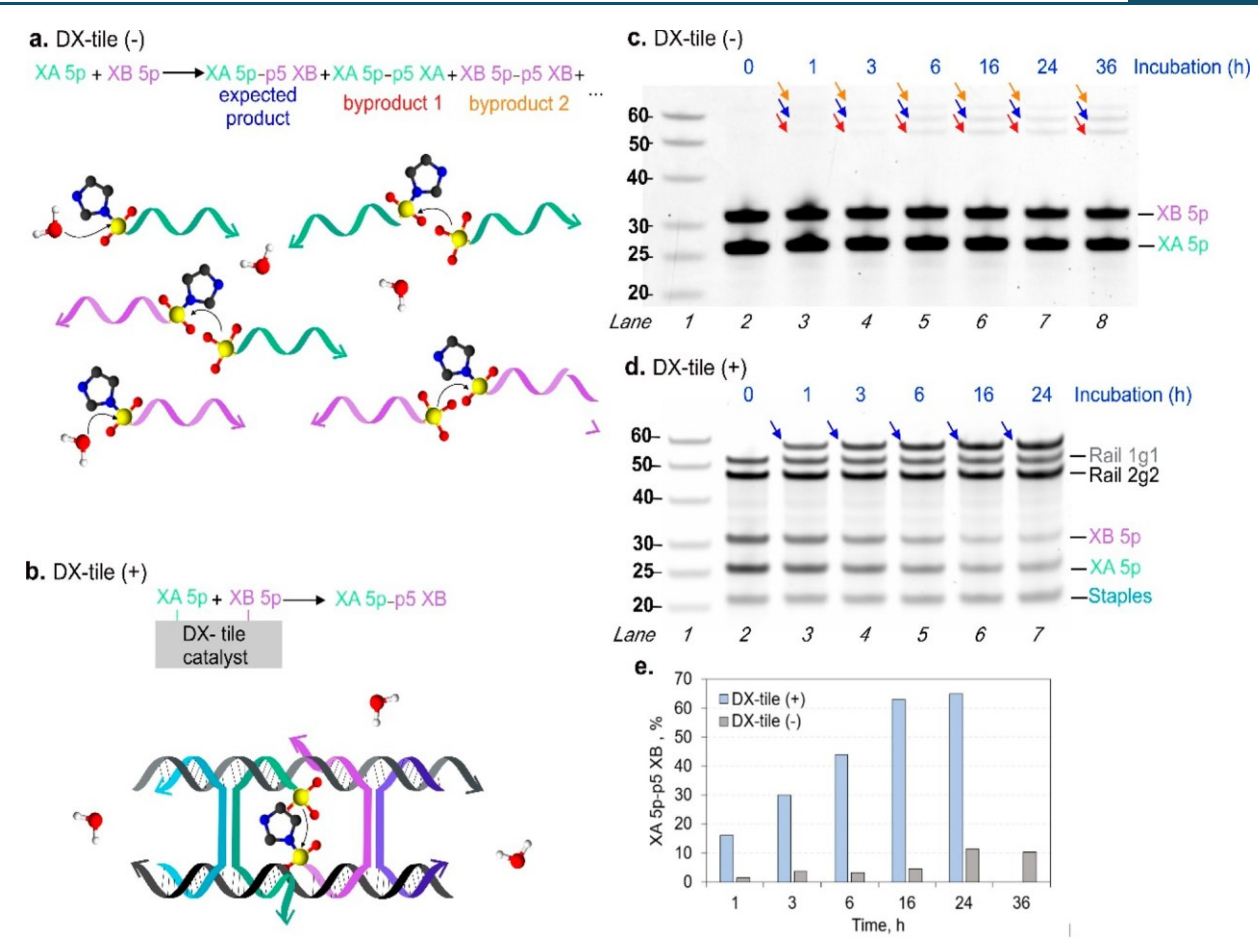


Figure 2. Comparison of uncatalyzed (DX-tile (-)) vs DX-tile-catalyzed (DX-tile (+)) chemical ligation of XA 5p and XB 5p. (a) Scheme of uncatalyzed chemical ligation. (b) Scheme of DX-tile-catalyzed chemical ligation. (c, d) PAGE analysis of the ligation products for (c) uncatalyzed and (d) DX-tile-catalyzed reactions. Lane 1: ssDNA ladder; Lane 2: prior cross-linking of 5' ends; Lanes 3–7 or 8: samples after ligation terminated at different incubation times (as indicated). Blue arrows indicate the ligated product XAp-pXB with the expected length of 57 nt. Orange and red arrows indicate byproducts of the reaction. (e) Comparison of the yields of the ligation reaction on DX tile (blue bars) and in solution (gray bars). The yield quantification was done as described in Methods.

attached to the ends of DNA strands. To illustrate the feasibility for DNA nanostructures to be used as catalysts, here we explored the 5'-5' chemical ligation of two oligonucleotides. Even though a 5'-5' phosphodiester bond is known in nature (e.g., found in mRNA cap structure), no known catalyst is capable of the 5'-5' ligation of two DNA strands of arbitrary sequences.

To achieve the 5′–5′ DNA ligation, we turned our attention to a DNA nanostructure called double-crossover antiparallel even (DAE) tile (also known as a DX tile) introduced by Fu and Seeman in 1993.¹¹ DX tile consists of five DNA strands (Figure 1b), which form two DNA helixes bound to each other via two DNA four-way junctions (crossovers). Figure 1c shows how a DX-tile-like nanostructure can be used as a template for bringing the 5′ ends of two nucleic acid strands (XA 5p and XB 5p) into proximity. In the present study, we demonstrate an enhancement in the reaction rate and yield of the chemical ligation and its specificity due to the proximity and orientation effect provided by the DX-tile-like structure. Our findings may become a step toward exploring DNA nanostructures for rational design of enzyme-like catalytic centers.

5'-5' and 3'-3' Chemical Ligation Catalyzed by DX Tile. First, we designed a 5'-5' DNA ligation system by forming a DX tile containing strands Rail 1, Rail 2 and four crossover

strands: XA 5p, XB 5p, staples 5 and 6 (Figure 1c). The sequence of the XA 5p and XB 5p oligonucleotides to be ligated were arbitrarily chosen with ~50% G/C content and absence of stable intramolecular secondary structures (Table S1). Both XA 5p and XB 5p were elongated with 3'-terminal oligo-T tails to be 26 and 31 nucleotides (nt), respectively, to have different electrophoretic mobilities and enable analysis of the tile formation and ligation reaction using polyacrylamide gel electrophoresis (PAGE). The sequences of the Rail 1 and Rail 2 strands included a 10 nt fragment complementary to both XA 5p and XB 5p. Similarly, they contained oligo-T tails of different lengths that could distinguish the strands' mobility in PAGE). Staples 5 and 6 were designed to bind Rail 1 and 2 strands at two DNA helical turns (21 nt) apart from each other to accommodate XA 5p and XB 5p in the middle of the tile (Figure 1c). In the resulting six-stranded complex, the 5' ends of XA 5p and XB 5p were positioned on the inner sides of the DNA helixes ("inside" the tile) in proximity to each other, as shown in Figure 2b. Therefore, their chemical ligation could take place right in the center of the nanostructure. The correct association of the six strands into the expected complex was confirmed by native PAGE analysis prior to cross-linking (Figure S1).

For the chemical ligation, we used the 1-cyanoimidazole (1-CNI) condensation system developed by Kanaya and Yanagawa, 12 which was shown to be effective for the 5'-3'templated ligation of oligoadenylates in aqueous solutions (Scheme S1). 12 Mn<sup>2+</sup>, Zn<sup>2+</sup>, Cu<sup>2+</sup>, Cd<sup>2+</sup>, Co<sup>2+</sup>, Ni<sup>2+</sup>, and Mg<sup>2+</sup> have been coupled with 1-CNI due to their influence in the ligation yield, with Mn<sup>2+</sup> and Zn<sup>2+</sup> most commonly used. <sup>13–15</sup> The reaction involves activation of the terminal phosphate with 1-CNI to facilitate its attack by a nucleophile. The reaction mechanism for phosphate activation<sup>12,13</sup> and divalent cation assisting the nucleophilic attack has been proposed and characterized.<sup>12,13,16</sup> We ran a series of optimization experiments to increase the yield of the DX-tile-assisted 5'-5'ligation. The 5' end of one strand was either phosphorylated (XA 5p) or lacked a phosphate group (XA), while the 5' end of another strand was always phosphorylated (XB 5p). To study the effect of the gap between the strands to be ligated, we left 1 or 2 nt single-stranded gaps, as shown in Figure 1c.

The best 5'-5' ligation yields were obtained when (i) both strands were 5'-end-phosphorylated (XA 5p + XB 5p, Figure S2A); (ii) Mn<sup>2+</sup> rather than Zn<sup>2+</sup> was used as a metal cofactor (Figure S2B), which aligns with previous reports;<sup>12,14</sup> (iii) at 37 °C rather than at 22 °C (Figure S3); (iv) at the optimal Mn<sup>2+</sup> concentration of 100 mM (Figure S3); and (v) the strands bound to both Rails 1 and 2 were separated by a 1 nt gap (Figure S4). Under the optimized conditions, the reaction reached a plateau within 16 h with a yield of  $\sim$ 65% producing no ligation side products (Figures 2d,e and S5). Furthermore, to increase the flexibility of the two reacting phosphate groups, we attached them to strands XA 5p and XB 5p via a flexible triethylene glycol spacer (iSp9). However, this did not improve the reaction yield (Figure S6).

In contrast, the uncatalyzed (DX-tile-free) ligation under similar conditions produced less than a 5% yield of the expected product after 16 h incubation. We observed a 2-fold yield increase after 24 h, but after 36 h the DX-tile-free ligation seemed to plateau (Figure 2c,e). The reaction rates for DX-tile and DX-tile-free ligation were calculated to be 0.40 ± 0.096 and 0.07 ± 0.019 µmol L<sup>-1</sup> h<sup>-1</sup>, respectively, indicating that DX tile enhances the reaction rate. In addition, two side products ◆52 nt XA−XA and 62 nt XB−XB • were formed in noticeable amounts in the absence of DX tile (Figure 2a,c, indicated by red and orange arrows, respectively). We therefore concluded that as a catalyst, the DX-tile-like association increases the ligation yield by ~12-fold and the

reaction rate by  $\sim$ 5.7-fold and improves the reaction specificity.

We also tested the possibility of bringing the ends of the two DNA strands together using a simpler arrangement than the DX tile, where Rail 1 and 2 strands were bound to each other directly (without staple strands) and formed a "bubble" with the sequences complementary to the strands to be cross-linked (Figure S8). However, such a system produced only ~7% yield of the ligation product, thus confirming the advantage of the DX tile as a template for chemical ligation.

The identified optimal conditions were also applied for the ligation of XA 3p and XB 3p strands to achieve the 3'-3' ligation of two DNA strands (Scheme S7). Under these conditions, the reaction reached a plateau within 16 h with a yield of 52% for the 3'-3' ligation products (Figure 3b, Lane 3). This ligation yield was lower than for the 5'-5' ligation product, most likely due to the lower reactivity of the secondary phosphate group and unassembled reacting strands

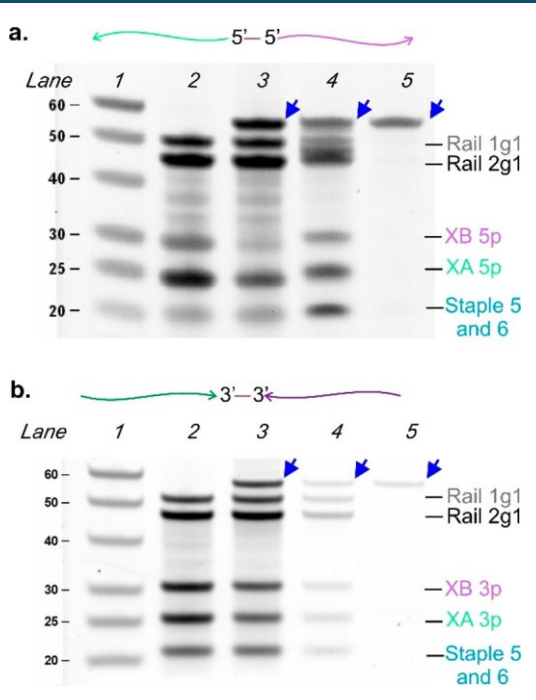


Figure 3. 12% dPAGE analysis of the synthesis and isolation steps for the (a) 5'-5' ligation products and (b) 3'-3' ligation product. Lane 1: ssDNA ladder (the sizes of the ladder bands are indicated to the left of the lane); Lane 2: DX tile prior to cross-linking; Lane 3: DX tile after the reaction (the 5'-5' and 3'-3' ligation yields are  $\sim 70\%$  and 52%, respectively); Lane 4: ligation reaction mixture prior to the digestion of the tile components by the exonuclease treatment; Lane 5: same as Lane 4 after the exonuclease treatment. Blue arrows indicate the cross-linking product XAp-pXB with the expected length of 57 nt.

(Figure S1b). However, we do not exclude the possibility that further optimization may improve the yield of the 3'-3' ligation.

Isolation of the Ligation Products. After the ligation reaction, the DNA strand with switched polarity remained in the mixture with other DX-tile-forming DNA strands. To isolate the ligation product, we added oligonucleotides that were fully complementary to the strands Rail 1g1 and 2g1, staples 5 and 6. This mixture was digested with Exo VIII, an exonuclease that degrades double-stranded DNA (dsDNA) in the 5' to 3' direction. We hypothesized that since the XA 5p-p5 XB ligation product did not have free 5' ends, it would remain resistant to the Exo VIII treatment.

Indeed, after treatment, we obtained a single DNA strand (Figure 3a, Lane 5), which could be further purified from Exo VIII by routine phenol extraction and ethanol precipitation. The size of the 5'-5' ligation product corresponds to the expected length (indicated by blue arrows in Figure 3a, Lanes 3–5). Similarly, we achieved isolation of the pure XA 3p-p3XB product upon treatment with Exo III, which degrades both dsDNA and ssDNA in the 3' to 5' direction. In this case, there was no need to add DNA strands complementary to Rail 1g1 and Rail 2g1 or the staple strands. Same as for the 5'-5'ligation product, the length of the 3'-3' product did not change during the enzymatic treatment, which indicates the absence of the free 3' ends and confirms the structure of the ligation product (Figure 3b, Lane 5). Therefore, the switched polarity feature of the ligation products makes them suitable for an easy isolation procedure that is affordable by even lowBioconjugate Chemistry pubs.acs.org/bc Communication

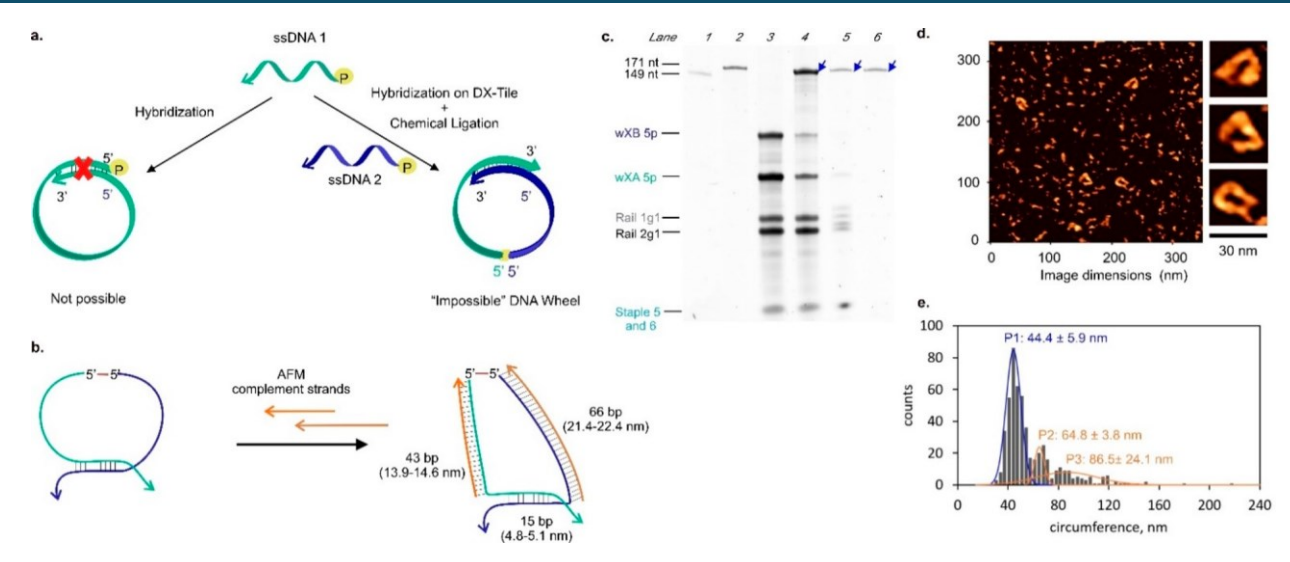


Figure 4. (a) Scheme comparing the structural requirements for the "impossible DNA wheel" structure. (b) Enforcement of the wXA 5p-p5 wXB assembly with the complementary strands to form a triangle-shaped impossible DNA wheel for AFM imaging. (c) 8% dPAGE run at 60 °C: Lane 1: 149 nt DNA marker; Lane 2: 171 nt DNA marker; Lane 3: impossible DNA wheel sample before the ligation reaction; Lane 4: same as Lane 3 after the reaction, yield  $69 \pm 4\%$ ; Lane 5: ligation product before Exo VIII treatment; Lane 6: ligation product after Exo VIII digestion. (d) Representative AFM image of the triangle-shaped impossible DNA wheel. (e) Gaussian distribution of the contour measurements (N = 521).

resource laboratories. Furthermore, both the purified and unpurified 5'-5' ligation products are stable at room temperature over 30 days (Figure S9).

Synthesis and Characterization of the "Impossible Wheel". DNA strands with switched polarity have been used for ligation of plasmid DNA via triplex formation, 17 as probes for nucleic acid analysis, 18,19 for the DNA-peptide library display system, 15 and to improve hemin-dependent peroxidase activity of Gquadruplexes.<sup>20</sup> However, to the best of our knowledge, such strands have not been explored by DNA nanotechnology, possibly due to the limited accessibility of this material. To illustrate the potential of DNA strands with switched polarity in DNA nanotechnology, we designed and synthesized a circular DNA nanostructure that we named an "impossible DNA wheel" (Figure 4a). This structure is impossible to create by plain intramolecular self-hybridization of a regular DNA oligonucleotide because of the parallel orientation of the DNA fragments in the double-stranded region (Figure 4a, left). However, it is possible to form the "impossible wheel" from a DNA strand with switched polarity (Figure 4a, right). In this work, we designed a DNA wheel to be 166 nt and formed by the 5'-5' ligation of 70 nt long wXA 5p and 96 nt long wXB 5p complementary to each other by 15 bp (60% GC). As a scaffold, we used the same DX tile system to hold the reacting strands wXA 5p and wXB 5p as was used in our prior experiments. Thus, synthesis of DNA wheels shorter or longer than 166 nt can be attempted using the same DX tile system if the DX tile binding site of both reacting strands is conserved. The reaction yield was  $68 \pm 4\%$  (Figure 4c, Lane 4), and isolation of the pure product was achieved by Exo VIII treatment (Figure 4c, Lane 6), as explained above.

To detect the "impossible DNA wheel" by atomic force microscopy (AFM), this structure was reshaped into a dsDNA triangle (Figure 4b) by adding two complementary strands, W1-Tri-A and W1-Tri-B (Table S1). This was needed to increase the rigidity and visibility of the structure in the AFM image. The triangle shape was visualized by AFM (Figure 4d). Based on the pitch of ds B-DNA (0.32–0.34 nm/bp), our impossible DNA wheel was estimated to have a circumference

of 40-42 nm in its triangular shape. To confirm the presence of the expected DNA wheel, contour measurements were performed on a population of 521 ring structures observed during AFM imaging (Figure S10). From the Gaussian distribution of the observed formations, three distinct populations were identified, with 385 of the structures falling under population P1 ( $44.4 \pm 5.9$  nm), which is closer to the expected circumference of 42 nm. We hypothesize that the observed broad range of sizes (P2 and P3) can be explained by the polymerization of the DNA wheel due to its self-complementarity (Figure 4b).

Discussion. DNA nanotechnology has introduced a number of sophisticated structures, many of which are being applied in biotechnology, gene therapy, and molecular computation. For example, the DX tile (Figure 1b), a more rigid building block than dsDNA, was used as a sensor for nucleic acid sequences (together with molecular beacon probes), 22,23 for assembling two-dimensional DNA crystals, DNA Sierpinski triangles, and hexagonal RNA nanotubes, among other applications. Here we used the DX tile in yet another role: as a catalyst for a chemical reaction. We hypothesized that the 2D structure of the DX tile can broaden the capabilities of the DNA-templated reactions explored earlier. 2-6

To illustrate the feasibility of using the DX tile as a catalyst, we synthesized 5'-5'- and 3'-3'-linked oligonucleotides of random sequences because of the practical significance of the reaction products as well as the absence of catalysts of these reactions. Such oligonucleotides can be prepared by the automated chemical nucleic acid synthesis using both conventional 3'-phosphoramidites and nonconventional and expensive 5'-phosphonamidites. 15,18,19 In practice, however, the synthesis of such strands requires a laboratory equipped with a DNA synthesizer, which makes such synthetic products unaffordable by an overwhelming majority of potential users. A DNA-templated synthesis of 5'-5'- and 3'-3'-linked oligonucleotides was reported by Chen et al., 15 who took advantage of the parallel duplex formation between poly-A and poly-T sequences. This method, however, puts a limitation on the choice of the sequences of oligonucleotides to be ligated: at

least one DNA strand must be poly-T or poly-A oligonucleotide

The DX-tile-assisted ligation uses only the proximity and orientation effect to achieve >12-fold yield enhancement and >5-fold reaction rate increase and, unlike the corresponding uncatalyzed reaction, results in no byproducts. Both yield enhancement and high reaction specificity are attributes of enzymatic catalysis. In this work, we did not explore multiple catalytic turnovers under the conditions when reactants are used in excess over the DX tile catalyst. Such reactions have been studied in the context of DNA- and RNA-templated synthesis and were reported to achieve up to 92 turnovers when optimized.<sup>27</sup> We also did not thoroughly optimize the 1-CNI chemistry (e.g., reagent concentrations, buffer, type of metal ion), since this was performed earlier using 3'-5'-templated oligonucleotide ligation and we just adopted the best conditions in this work.<sup>12,13,16</sup>

While developing this technique, we noticed that the ligation yield was significantly improved when both reacting strands had phosphorylated ends, in comparison with the earlier systems having only one strand phosphorylated. This higher reactivity can be explained both by a greater probability for the reactants to be activated by 1-cyanoimidazole as well as greater nucleophilicity of the phosphate group in comparison with the hydroxyl group under the reaction conditions. The ligation products in this case contained a phosphoanhydride instead of a regular phosphodiester linkage, which raised a question regarding its chemical stability in aqueous solutions. However, we did not observe degradation of the ligation product over 30 days at 22 °C and pH 7.4 (Figure S9).

For downstream applications, oligonucleotides with switched polarity obtained via DX-tile-assisted ligation may need to be isolated from the mixture of the DX-tile-forming strands, which would traditionally require HPLC or gel electrophoresis. To avoid a tedious purification procedure, we took advantage of the absence of free 5' ends in the 5'-5'ligation product or free 3' ends in the 3'-3' ligation products and treated the reaction mixtures with either 5'- or 3'exonuclease that would degrade all DNA present except the ligation products. This experiment highlights the improved nuclease resistance of the 5'-5' and 3'-3' oligonucleotides and inspires follow-up exploration of nonostructures built from DNA with inversed polarity in intracellular environment. Furthermore, we demonstrated that the ligation approach is applicable to form oligonucleotides with switched polarities of different lengths. Indeed, we used the DX-tile-assisted ligation to synthesize a 166 nt long "impossible DNA wheel" structure. We hope that the high ligation yield, applicability to any nucleic acid sequences, and simple purification procedure will make the reported synthetic scheme useful in laboratory practice.

It is worth noting that the DX-like structure can accommodate up to four functional groups in the middle if both 3' and 5' strands of XA and XB are functionalized. Some of the functional groups can act as catalysts, while others - as reagents. This would create a more sophisticated functional group arrangement, which may enable exploration of several catalytic strategies to mimic natural enzymes. Other structures that allow bringing together more than four groups, such as 5-, 8-, and 12-way DNA junctions, 28,29 can be explored for building even more sophisticated catalytic sites.

Conclusions. We demonstrated that a DNA nanostructure can be used to facilitate reactions not achievable by any known

enzyme. DNA strands of arbitrary sequences can be joined together by their 3'-3' or 5'-5' ends with the rate and yield enhancements of more than 5- and 12-fold, respectively, and greater specificity than that for the uncatalyzed reaction. This was achieved due to the proximity and orientation catalytic strategy provided by the DXtile scaffold. Building catalytic centers by attaching functional groups to specific positions in DNA nanostructures can become a new strategy for the rational design of artificial catalysts.

## **METHODS**

DX Tile Assembly and Chemical Ligation Reactions. DNA oligonucleotides comprising the DX tile complex were mixed at 20 µM in a buffer containing 200 mM imidazole-HCl (pH 6.5) and 75 mM MgCl<sub>2</sub>. The DX tile samples were annealed by denaturing the strands at 95 °C for 2 min and cooling to 22 °C over the period of 8 h. For the cross-linking reaction, 1-cyanoimidazole and MnCl<sub>2</sub> were added to the annealed samples to their final concentrations of 30 and 100 mM, respectively, and the reaction mixtures were incubated at 37 °C for 16 h unless otherwise specified.

AFM Imaging. AFM samples were prepared as follows: wXA 5p-wXB 5p ligation product was associated with AFM complementary strands (Table S1) in an assembly buffer (10 mM Tris-HCl, pH 7.4, and 2 mM MgCl<sub>2</sub>) followed by gel isolation of the complex and its resuspension in the assembly buffer. Mica substrates were modified with 1-(3-aminopropyl)silatrane (APS) to create a positively charged surface for deposition of DNA-DNA and RNA-DNA hybrid structures via electrostatic attraction between the negatively charged DNA backbone and positively charged APS-mica. Five microliters of each sample was deposited on the APS-modified mica and incubated for 2 min before rinsing the excess DNA with DI water. Optimal sample concentration ranged from 10-100 nM to avoid overlapping of DNA structures. Mica samples were dried under a flow of ultrahigh-purity argon gas and incubated overnight under vacuum before imaging. AFM images were obtained using a Multimode AFM Nanoscope IV system (Bruker Instruments, Santa Barbara, CA) operating in tapping mode in air with a RTESPA-300 AFM probe.

# ASSOCIATED CONTENT

## Supporting Information

The Supporting Information is available free of charge at https://pubs.acs.org/doi/10.1021/acs.bioconjchem.3c00502.

Materials, additional experimental procedures, sequences of oligonucleotides, and supporting data (PDF)

### **AUTHOR INFORMATION**

## **Corresponding Author**

Dmitry M. Kolpashchikov — Chemistry Department and Burnett School of Biomedical Sciences, University of Central Florida, Orlando, Florida 32816, United States; National Center for Forensic Science, University of Central Florida, Orlando, Florida 32816, United States; orcid.org/0000-0002-8682-6553; Email: Dmitry.Kolpashchikov@ucf.edu

#### **Authors**

Andrea C. Bardales — Chemistry Department, University of Central Florida, Orlando, Florida 32816, United States Joseph R. Mills — Chemistry Department, University of Central Florida, Orlando, Florida 32816, United States Complete contact information is available at: https://pubs.acs.org/10.1021/acs.bioconjchem.3c00502

#### **Author Contributions**

A.C.B. designed and conducted experiments, analyzed and prepared data for publication, and wrote the paper. J.R.M. carried out experiments, analyzed data, and contributed to the discussion and manuscript preparation, D.M.K. conceived the idea, designed research, analyzed data, and wrote the paper.

#### Notes

The authors declare no competing financial interest.

# A

### **ACKNOWLEDGMENTS**

We are grateful to Yuri L. Lyubchenko and Alexander Lushnikov for AFM imaging and analysis performed at the Nanoimaging Core Facility, University of Nebraska Medical Center, and Yulia V. Gerasimova for the fruitful discussion and corrections. This work was supported by the National Science Foundation through the CCF: Software and Hardware Foundations under Cooperative Agreements SHF-1907824 and SHF-2226021.

#### **DEDICATION**

This study is dedicated to the memory of the late Prof. Nadrian C. Seeman, the inventor of DNA nanotechnology, and the 30th anniversary of the first report on DX tile (Fu, T.-J.; Seeman, N.C. *Biochemistry* 1993, *32*, 3211–3220).

# REFERENCES

- (1) Voet, D.; Voet, J. G.; Pratt, C. W. Fundamentals of Biochemistry: Life at the Molecular Level; John Wiley & Sons, 2016.
- (2) Kanan, M. W.; Rozenman, M. M.; Sakurai, K.; Snyder, T. M.; Liu, D. R. Reaction Discovery Enabled by DNA-Templated Synthesis and in Vitro Selection. *Nature* 2004, *431*, 545–549.
- (3) Ma, Z.; Taylor, J.-S. Nucleic Acid-Triggered Catalytic Drug Release. *Proc. Natl. Acad. Sci. U. S. A.* 2000, 97, 11159–11163.
- (4) Houska, R.; Stutz, M. B.; Seitz, O. Expanding the Scope of Native Chemical Ligation Templated Small Molecule Drug Synthesis via Benzanilide Formation. *Chem. Sci.* 2021, *12*, 13450—13457.
- (5) Kolpashchikov, D. M. Binary Probes for Nucleic Acid Analysis. *Chem. Rev.* 2010, *110*, 4709–4723.
- (6) O'Reilly, R. K.; Turberfield, A. J.; Wilks, T. R. The Evolution of DNA-Templated Synthesis as a Tool for Materials Discovery. *Acc. Chem. Res.* 2017, *50*, 2496–2509.
- (7) Seeman, N. C.; Kallenbach, N. R. Design of Immobile Nucleic Acid Junctions. *Biophys. J.* 1983, *44*, 201–209.
- (8) Zhang, X.; Yan, H.; Shen, Z.; Seeman, N. C. Paranemic Cohesion of Topologically-Closed DNA Molecules. *J. Am. Chem. Soc.* 2002, 124, 12940–12941.
- (9) Liu, D.; Wang, M.; Deng, Z.; Walulu, R.; Mao, C. Tensegrity: Construction of Rigid DNA Triangles with Flexible Four-Arm DNA Junctions. *J. Am. Chem. Soc.* 2004, *126*, 2324–2325.
- (10) Jones, M. R.; Seeman, N. C.; Mirkin, C. A. Programmable Materials and the Nature of the DNA Bond. *Science* 2015, 347, No. 1260901.
- (11) Fu, T. J.; Seeman, N. C. DNA Double-Crossover Molecules. *Biochemistry* 1993, 32, 3211–3220.
- (12) Kanaya, E.; Yanagawa, H. Template-Directed Polymerization of Oligoadenylates Using Cyanogen Bromide. *Biochemistry* 1986, 25, 7423–7430.
- (13) Okita, H.; Kondo, S.; Murayama, K.; Asanuma, H. Rapid Chemical Ligation of DNA and Acyclic Threoninol Nucleic Acid (aTNA) for Effective Nonenzymatic Primer Extension. *J. Am. Chem. Soc.* 2023, *145*, 17872–17880.

- (14) Ferris, J. P.; Huang, C.-H.; Hagan, W. J. N-Cyanoimidazole and Diimidazole Imine: Water-Soluble Condensing Agents for the Formation of the Phosphodiester Bond. *Nucleosides Nucleotides* 1989, 8, 407–414.
- (15) Chen, H.; Du, F.; Chen, G.; Streckenbach, F.; Yasmeen, A.; Zhao, Y.; Tang, Z. Template-Directed Chemical Ligation to Obtain 3'-3' and 5'-5' Phosphodiester DNA Linkages. *Sci. Rep.* 2014, *4*, 4595.
- (16) Yi, R.; Hongo, Y.; Fahrenbach, A. C. Synthesis of Imidazole-Activated Ribonucleotides Using Cyanogen Chloride. *Chem. Commun.* 2018, *54*, 511–514.
- (17) Kandimalla, E. R.; Agrawal, S. Hoogsteen DNA Duplexes of 3'-3'- and 5'-5'-Linked Oligonucleotides and Triplex Formation with RNA and DNA Pyrimidine Single Strands: Experimental and Molecular Modeling Studies. *Biochemistry* 1996, *35*, 15332–15339.
- (18) Zhou, T.; Chen, G.; Wang, Y.; Zhang, Q.; Yang, M.; Li, T. Synthesis of Unimolecularly Circular G-Quadruplexes as Prospective Molecular Probes. *Nucleic Acids Res.* 2004, *32*, No. e173.
- (19) Kandimalla, E. R.; Agrawal, S. 'Cyclicons' as Hybridization-Based Fluorescent Primer-Probes: Synthesis, Properties and Application in Real-Time PCR. *Bioorg. Med. Chem.* 2000, 8, 1911–1916.
- (20) Cao, Y.; Ding, P.; Yang, L.; Li, W.; Luo, Y.; Wang, J.; Pei, R. Investigation and Improvement of Catalytic Activity of G-Quadruplex/Hemin DNAzymes Using Designed Terminal G-Tetrads with Deoxyadenosine Caps. *Chem. Sci.* 2020, *11*, 6896–6906.
- (21) Zagorski, K.; Stormberg, T.; Hashemi, M.; Kolomeisky, A. B.; Lyubchenko, Y. L. Nanorings to Probe Mechanical Stress of Single-Stranded DNA Mediated by the DNA Duplex. *Int. J. Mol. Sci.* 2022, 23, 12916.
- (22) Kolpashchikov, D. M.; Gerasimova, Y. V.; Khan, M. S. DNA nanotechnology for nucleic acid analysis: DX motif-based sensor. *ChemBioChem* 2011, *12*, 2564–2567.
- (23) Cornett, E. M.; Campbell, E. A.; Gulenay, G.; Peterson, E.; Bhaskar, N.; Kolpashchikov, D. M. Molecular logic gates for DNA analysis: detection of rifampin resistance in M. tuberculosis DNA. *Angew. Chem., Int. Ed.* 2012, *51*, 9075–9077.
- (24) Winfree, E.; Liu, F.; Wenzler, L. A.; Seeman, N. C. Design and Self-Assembly of Two-Dimensional DNA Crystals. *Nature* 1998, *394* (6693), 539–544.
- (25) Rothemund, P. W. K.; Papadakis, N.; Winfree, E. Algorithmic Self-Assembly of DNA Sierpinski Triangles. *PLoS Biol.* 2004, 2, No. e424.
- (26) Naskar, S.; Joshi, H.; Chakraborty, B.; Seeman, N. C.; Maiti, P. K. Atomic Structures of RNA Nanotubes and Their Comparison with DNA Nanotubes. *Nanoscale* 2019, *11*, 14863–14878.
- (27) Abe, H.; Kool, E. T. Destabilizing Universal Linkers for Signal Amplification in Self-Ligating Probes for RNA. *J. Am. Chem. Soc.* 2004, *126*, 13980–13986.
- (28) Kadrmas, J. L.; Ravin, A. J.; Leontis, N. B. Relative Stabilities of DNA Three-Way, Four-Way and Five-Way Junctions (Multi-Helix Junction Loops): Unpaired Nucleotides Can Be Stabilizing or Destabilizing. *Nucleic Acids Res.* 1995, *23*, 2212–2222.
- (29) Wang, X.; Seeman, N. C. Assembly and Characterization of 8-Arm and 12-Arm DNA Branched Junctions. *J. Am. Chem. Soc.* 2007, 129, 8169—8176.